Inorganic Chemistry

Article

pubs.acs.org/IC

# Pore Design of Two-Dimensional Coordination Polymers toward Selective Adsorption

Yuh Hijikata,[†] Satoshi Horike,[†,‡] Masayuki Sugimoto,[†] Munehiro Inukai,[§] Tomohiro Fukushima,[†] and Susumu Kitagawa*[,†,§,⊥]

[†]Department of Synthetic Chemistry and Biological Chemistry, Graduate School of Engineering, Kyoto University, Katsura, Nishikyo-ku, Kyoto 615-8510, Japan

[‡]PRESTO, Japan Science and Technology Agency, 4-1-8 Honcho, Kawaguchi, Saitama 332-0012, Japan

[§]Institute for Integrated Cell-Material Sciences (WPI-iCeMS), Kyoto University, Yoshida, Sakyo-ku, Kyoto 606-8501, Japan

[⊥]ERATO, Kitagawa Integrated Pores Project, Japan Science and Technology Agency, Kyoto Research Park Building No. 3, Shimogyo-ku, Kyoto 600-8815, Japan

Supporting Information

**ABSTRACT:** We have synthesized four porous coordination polymers (PCPs) using $Zn^{2+}$, 4,4′-sulfonyldibenzoate (sdb), and four types of dinitrogen linker ligands, 1,4-diazabicyclo[2,2,2]octane (dabco), 1,4-bis(4-pyridyl)benzene (bpb), 3,6-bis(4-pyridyl)-1,2,4,5-tetrazine (bpt), and 4,4′-bipyridyl (bpy). The bent sdb ligands form a rhombic space connected by zinc paddle-wheel units to form a one-dimensional double chain, and each dinitrogen ligand linked the one-dimensional double chains. There are different assembled structures of two-dimensional sheets with the same connectivities between $Zn^{2+}$ and the organic ligands. $[Zn_2(sdb)_2(dabco)]_n$ (**1**) has a noninterpenetrated and noninterdigitated structure, $[Zn_2(sdb)_2(bpb)]_n$ (**2**) and $[Zn_2(sdb)_2(bpt)]_n$ (**3**) have interdigitated structures, and $[Zn_2(sdb)_2(bpy)]_n$ (**4**) has an interpenetrated structure. The length of the dinitrogen ligands dominated their assembled structures and flexibility, which influence the adsorption properties. The flexible frameworks of **2** and **3** provide different stepwise adsorption behaviors for $CO_2$, $CH_4$, $C_2H_6$, and $C_2H_4$ affected by their pore diameters and the properties of the gases. Their different adsorption properties were revealed by IR spectroscopy and X-ray analysis under a gas atmosphere. The framework of **4** possesses less flexibility and a smaller void space than the others and a negligible amount of $CH_4$ was adsorbed; however, **4** can adsorb either $C_2H_6$ or $C_2H_4$ through the gate-opening phenomenon. Measurement of the solid-state $^2H$ NMR was also carried out to investigate the relationship between the framework structure and the dynamics of bpy with regard to the lower flexibility of **4**. We have demonstrated a strategy to control the pore size and assembled structures toward selective adsorption properties of PCPs.

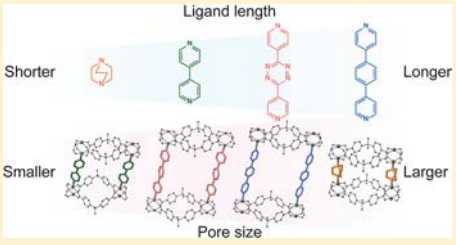


## INTRODUCTION

Porous coordination polymers (PCPs) or metal−organic frameworks have emerged as a new class porous materials since the end of 1990s.[1] PCPs are constructed from organic ligands and metal ions, and unlimited combinations of ligands and metals provide various structures.[2] These frameworks have been investigated as functional materials for storage,[3] separation,[4] reaction fields,[5] sensors,[6] and transport.[7] Their gas-adsorption properties have been focused on in particular, and various structures have been developed not only to enhance storage capacities but also to improve the selectivity of adsorption using their intrinsic flexible connectivity derived from the moderate strength of the coordination bonds.[8] This flexibility is also an attractive property compared with other rigid porous materials such as zeolite or mesoporous silica.[9] While frameworks connected three-dimensionally sometimes show structural changes based on the flexible coordination bond, other interpenetrated three-dimensional (3D) frameworks and assembled structures of two-dimensional (2D) sheets have overall structural flexibility.[4a,10] Overall structural flexibility means that the relative positions of neighboring frameworks change. In particular, 2D frameworks often show selective adsorption or gate-opening adsorption phenomena based on the expansion of 2D sheets.[10b,c] From a synthetic point of view, several series of 3D frameworks have been synthesized systematically with various ligands,[11] different divalent metals,[12] trivalent metals,[13] or both variant ligands and metals.[8b,14] In contrast, only a few series of 2D assembled frameworks are known.[10c,15] One of the series of 2D frameworks, which are called coordination polymers with interdigitated structures (CIDs), has been developed.[16] CIDs are constructed from metal ions, linker dinitrogen ligands, and dicarboxylate ligands bent at ca. 120°, for instance, isophthalate derivatives. Many 2D assembled structures have different adsorption behaviors, such as stepwise, selective, and gate-opening adsorption as a result of their structural flexibility.

**Received:** September 14, 2012
**Published:** March 15, 2013

   dx.doi.org/10.1021/ic302006x | Inorg. Chem. 2013, 52, 3634−3642

On the basis of this strategy, we synthesized four 2D frameworks constructed from $Zn^{2+}$ and investigated their adsorption properties. We chose 4,4′-sulfonyldibenzoic acid ($H_2$sdb) bent at ca. 90°,[17] instead of the isophthalic acids. Four types of dinitrogen ligands, 1,4-diazabicyclo[2,2,2]octane (dabco), 1,4-bis(4-pyridyl)benzene (bpb), 3,6-bis(4-pyridyl)-1,2,4,5-tetrazine (bpt), and 4,4′-bipyridyl (bpy), were selected as linkers for the one-dimensional (1D) double chains consisting of $Zn^{2+}$ and sdb. The linked chains expand to 2D sheets. The length of the linker ligands determined the 2D sheet assembly and their pore size. X-ray analysis showed that one of them is a noninterpenetrated and noninterdigitated structure, two of them are interdigitated structures, and the other is an interpenetrated structure; however, all four frameworks have the same connectivity. We measured the solid-state $^2$H NMR spectrum for the bpy-linked compound to obtain information relating to the interpenetrated structure and the dynamics of spatially isolated bpy. Gas-adsorption measurements of $CO_2$, $CH_4$, $C_2H_6$, and $C_2H_4$ were performed to determine how the adsorption behavior depends on the framework. Stepwise adsorptions of interdigitated structures were revealed by the combination of X-ray analysis and IR spectroscopy under a gas atmosphere. We also investigated the gate-opening behavior and selective adsorption of the interpenetrated structure. In addition, we carried out adsorption measurements up to $P$ = 0.9 MPa to examine their selectivity at room temperature. In this work, we have demonstrated rational synthesis using sdb and dinitrogen linker ligands toward selective adsorption.

## EXPERIMENTAL SECTION

**Materials.** All chemicals and solvents from Wako Pure Chemical Industries, Ltd., and Tokyo Chemical Industry Co., Ltd., used in the syntheses were of reagent-grade and were used without further purification. Ligands of 1,4-diazabicylo[2.2.2]octane (dabco), 3,6-bis(4-pyridyl)-1,2,4,5-tetrazine (bpt), 4,4′-bipyridyl (bpy), 4,4′-sulfonyldibenzoic acid ($H_2$sdb), and $Zn(NO_3)_2{\cdot}6H_2O$ were obtained. 1,4-Bis(4-pyridyl)benzene (bpb) was prepared according to a previous report.[18]

**Synthesis of $[Zn_2(sdb)_2(dabco)]_n$ (1).** dabco (0.4 mmol, 44.9 mg), $H_2$sdb (0.8 mmol, 245 mg), and $Zn(NO_3)_2{\cdot}6H_2O$ (0.8 mmol, 238 mg) were dissolved in *N*,*N*-dimethylformamide (DMF; 40 mL). The solution was sealed in a glass vial and heated at 100 °C for 2 days. After cooling and filtration, white powder crystals of **1**⊃solvent were obtained (56% yield). The crystals were heated at 150 °C in vacuo for 6 h to remove the solvent molecules. We could not determine the kinds of solvent guest molecules experimentally. Elem anal. Calcd for **1** $[Zn_2(C_{14}H_8SO_6)_2(C_6H_{12}N_2)]_n$: C, 47.73; H, 3.77; N, 3.27. Found for **1**⊃solvents $\{[Zn_2(C_{14}H_8SO_6)_2(C_6H_{12}N_2)]\cdot(solvents)_n\}$: C, 46.81; H, 4.74; N, 6.16.

**Synthesis of $[Zn_2(sdb)_2(bpb)]_n$ (2).** bpb (0.4 mmol, 92.9 mg), $H_2$sdb (0.8 mmol, 245 mg), and $Zn(NO_3)_2{\cdot}6H_2O$ (0.8 mmol, 238 mg) were dissolved in DMF (40 mL). The solution was sealed in a glass vial and heated at 80 °C for 2 days. After cooling and filtration, white powder crystals of **2**⊃DMF were obtained (78% yield). The crystals were heated at 150 °C in vacuo for 6 h to remove the solvent of DMF. Elem anal. Calcd for **2**⊃DMF $\{[Zn_2(C_{14}H_8SO_6)_2(C_{16}H_{12}N_2)]\cdot 2.5DMF_n\}$: C, 53.58; H, 3.97; N, 5.46. Found: C, 53.29; H, 3.80: N, 5.47.

**Synthesis of $[Zn_2(sdb)_2(bpt)]_n$ (3).** bpt (1.2 mmol, 283 mg), $H_2$sdb (0.8 mmol, 245 mg), and $Zn(NO_3)_2{\cdot}6H_2O$ (0.8 mmol, 238 mg) were dissolved in DMF (40 mL). The solution was sealed in a glass vial and heated at 100 °C for 2 days. After cooling and filtration, red powder crystals of **3**⊃DMF were obtained (68% yield). The crystals were heated at 100 °C in vacuo for 6 h to remove the solvent of DMF. Elem anal. Calcd for **3**⊃DMF $\{[Zn_2(C_{14}H_8SO_6)_2(C_{12}H_8N_6)]\cdot 2.5DMF_n\}$: C, 49.25; H, 3.61; N, 10.28. Found: C, 48.74; H, 3.48; N, 10.28.

**Synthesis of $[Zn_2(sdb)_2(bpy)]_n$ (4).** bpy (0.4 mmol, 62.4 mg), $H_2$sdb (0.8 mmol, 245 mg), and $Zn(NO_3)_2{\cdot}6H_2O$ (0.8 mmol, 238 mg) were dissolved in DMF (40 mL). The solution was sealed in a glass vial and heated at 100 °C for 2 days. After cooling and filtration, white powder crystals of **4** were obtained (75% yield). The crystals were heated at 150 °C in vacuo for 3 h to confirm the absence of solvents. Elem anal. Calcd for **4** $\{[Zn_2(C_{14}H_8SO_6)_2(C_{10}H_8N_2)]_n\}$: C, 50.96; H, 2.70; N, 3.13. Found: C, 49.82; H, 2.77; N, 3.42.

**Synthesis of $[Zn_2(sdb)_2(bpy\text{-}d_8)]_n$ (4-*d*).** **4**-*d* was synthesized in the same way to obtain **4** using deuterated bpy (bpy-$d_8$) instead of nondeuterated bpy. Bpy-$d_8$ was synthesized following a previous report.[19]

**Single-Crystal X-ray Measurements.** Data were recorded on a Rigaku/MSC Saturn CCD diffractometer with confocal monochromated Mo $K_\alpha$ radiation ($\lambda$ = 0.7107 Å) and processed using the *CrystalClear* program (Rigaku). The structure of **1** was solved by direct methods (*SIR2002*) and refined by full-matrix least-squares refinement using the *CRYSTALS* computer program. The structures of **2**−**4** were solved by direct methods (*SIR97*) and refined by full-matrix least-squares refinement using the *SHELXL-97* computer program. The positions of non-H atoms were refined with anisotropic displacement factors. The H atoms were refined geometrically, using a riding model. The void volumes of each framework were estimated by the *PLATON* program.[20] While the framework structure of **1** was refined easily, the solvent molecules in **1** could not be refined because of their highly disordered structure. Therefore, *SQUEEZE* function of the *PLATON* program was used to eliminate the contribution of the electron density in the solvent region from the intensity data.[21] The contribution of these species was removed, and final refinement was performed. CCDC reference numbers are 901390−901394. These data can be obtained free of charge from The Cambridge Crystallographic Data Center via www.ccdc.cam.ac.uk/data_request/cif.

**Other Physical Measurements.** Elemental analyses were carried out on a Flash EA 1112 series Thermo Finnigan instrument. Thermogravimetric analyses (TGA) were carried out with a Rigaku Thermo Plus TG-8120 instrument under a nitrogen atmosphere and at a heating rate of 10 K·min$^{-1}$ from 298 to 773 K. The powder X-ray diffractions (PXRD) were recorded with a Rigaku RINT-2200HF (Ultima) diffractometer equipped with Cu $K_\alpha$ radiation ($\lambda$ = 1.54 Å). The synchrotron-radiation PXRD patterns of **3** and **4** were measured with a large Debye−Scherrer camera, with imaging plates as detectors on the BL02B2 beamline at the Super Photon ring-8 (SPring-8). Powder of the sample was put in a silica glass capillary under controlled $CO_2$ pressure and temperature. The radiation wavelength was 0.80035 Å. The adsorption isotherms of $CO_2$, $CH_4$, $C_2H_4$, and $C_2H_6$ were measured at 195 and 298 K using a BELSORP mini-instrument and BELSORP-HP instrument from BEL Japan, Inc., respectively. IR spectra were measured using a Thermo Fisher scientific Nicolet 6700 spectrometer, and the pressure of $CO_2$ was controlled. The $^1$H NMR measurements were carried out with a JEOL A-500 spectrometer operating at 500 MHz. Solid-state $^2$H NMR spectra were measured under vacuum in 9.4 T, and the spectra were recorded with a Bruker AVANCE III instrument.

## RESULTS AND DISCUSSION

**Porous Structures of Compounds.** We synthesized solvothermally four PCPs constructed from $Zn^{2+}$sdb with dinitrogen linker ligands dabco, bpb, bpt, and bpy. Their crystal structures in the as-synthesized phase were determined by single-crystal X-ray diffraction analysis at 223 K, which showed that they have different assembled structures of 2D sheets with the same connectivity. The crystal structure of **1**⊃solvent shows that the carboxy groups in the four sdb ligands connected to two $Zn^{2+}$ ions to form paddle-wheel units. The sdb ligands are bent at ca. 90°, and they form rhombus grids linked by the paddle wheel to form a 1D double chain, as shown in Figure


dx.doi.org/10.1021/ic302006x | Inorg. Chem. 2013, 52, 3634−3642

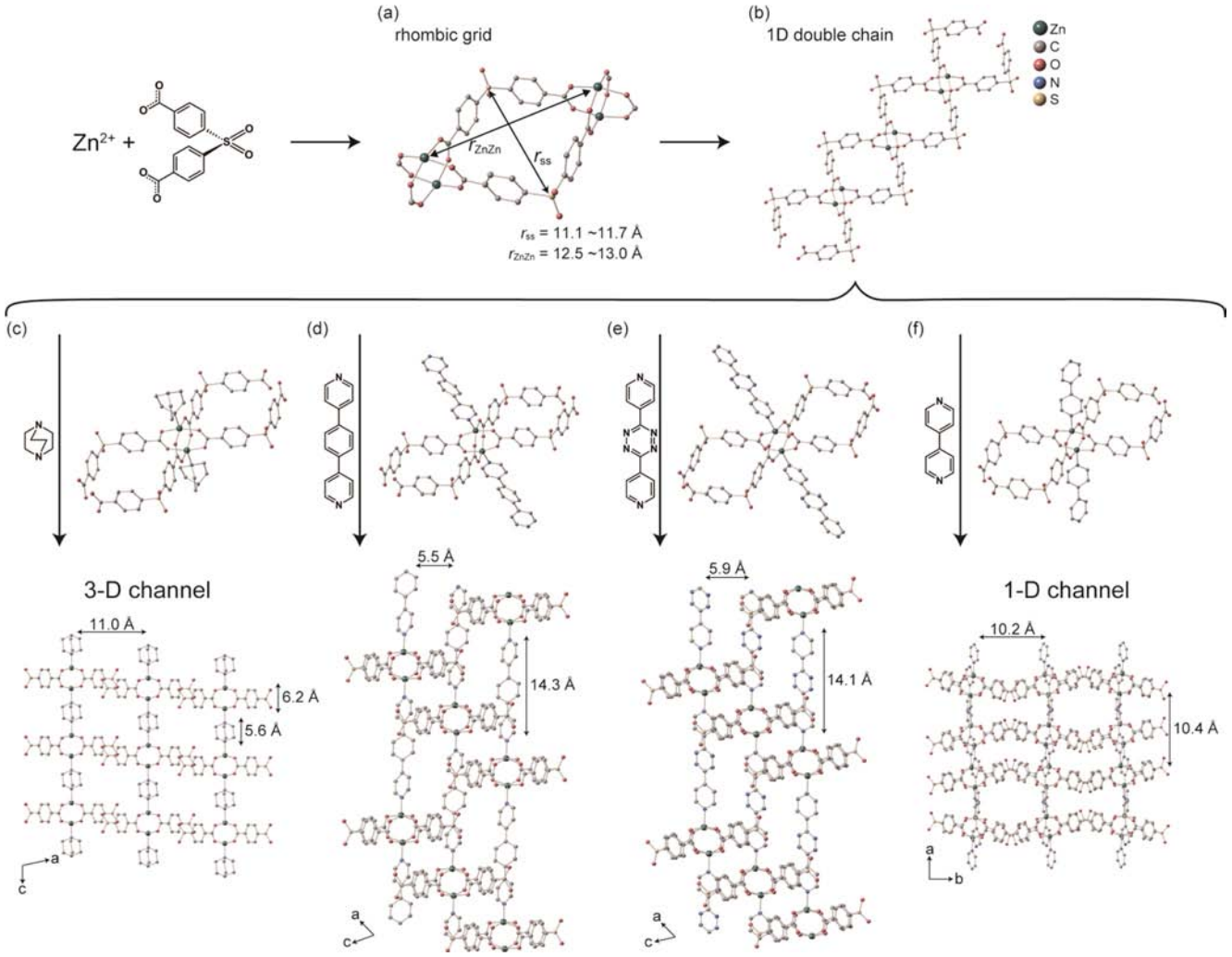


**Figure 1.** Schematic description of the structural component of the rhombic grid (a) and 1D double chain (b) and assembled crystal structures of **1**–**4** (c–f) without H atoms and guest solvent molecules for clarity.

1a,b. There is enough space for gas molecules to be adsorbed or to pass through the 1D double chain, which is different from the 1D chains in the series of CIDs.[16] The two $Zn^{2+}$ ions in the paddle-wheel units are linked axially by dabco ligands, and then the 2D sheet is extended. The 2D sheets assemble to form the 3D porous structure. Figure 1c shows the crystal structure of **1**⊃solvent. The distance between 1D double chains along the *c* axis is the shortest (5.6 Å) among the four frameworks because of the shortest distance between the N atoms in dabco. The height of the sdb ligand is 6.2 Å, and it is difficult to interdigitate or interpenetrate because the height is longer than the distance between the 1D double chains linked by dabco. The void volume of **1** is the largest among the four frameworks, 45.8%. The framework of **1** is assembled via $\pi-\pi$ interaction of sdb between neighboring 2D sheets, in which the distance is 3.6 Å. While dabco constructs a permanent pore without interdigitation and interpenetration, two longer linker ligands, bpb or bpt, provided different assembled structures from **1** with the same connectivities. The crystal structures of **2**⊃DMF and **3**⊃DMF are shown in Figure 1d,e. Although the central aromatic rings in bpb and bpt are different, the distance between their N atoms is similar, 11.3 and 11.1 Å, respectively. These two longer ligands are able to construct interdigitated structures; therefore, both **2** and **3** form similar interdigitated structures. The dihedral angle of the central benzene and pyridyl rings in **2** is 25.7°, and the angle of the tetrazine and pyridyl rings in **3** is 9.7°. These angles are comparable to the reported 2D frameworks,[16p] in which the larger angle is distorted by steric hindrance between protons on the central benzene and pyridyl rings in bpb. The void volumes of **2** and **3** are similar, 32.5% and 32.8%, respectively. While those void volumes are smaller than that of **1** because interdigitation reduces the void space in 2D sheets, they are prospective structures for stepwise adsorption behaviors through structural changes that allow gas molecules to be accommodated. The three frameworks of **1**–**3** have rhombic grid pores of sdb, ca. 11.0 Å × 13.0 Å in 2D sheets. The grids form a 1D pore in **1** along the dabco ligands. In the cases of **2** and **3**, the grids were overlapped partially by sulfonyl groups of sdb in neighboring 2D sheets. When bpy was used to construct the framework with the same connectivity as the other three frameworks, the rhombic grids were occupied by bpy to form the interpenetrated structure in 2D sheets. Analogous structures of **4** including a guest $H_2O$ molecule have been reported, and they are composed of $Zn^{2+}$, $Cu^{2+}$, and $Ni^{2+}$ ions.[22] The distance between the N atoms in bpy is 7.0 Å, which is an intermediate length in the four linker ligands and longer than the height of sdb. The assembled structure of **4** is shown in Figure 1f. The


dx.doi.org/10.1021/ic302006x | *Inorg. Chem.* 2013, 52, 3634–3642

void volume of **4** is smallest, 9.1%, among the four frameworks, and it constructs a narrow 1D pore, 3.3 Å × 6.9 Å along the *c* axis using bpy to occupy the rhombic grid.

**Thermal Stability and Evaluation of the Structural Flexibility.** We carried out TGA measurements to determine the amount of guest molecules included in the as-synthesized phase of each framework or to confirm the absence of solvents. PXRD measurements were also performed at 298 K to investigate the structural flexibility of frameworks before and after desolvation of guests. The measured PXRD patterns and TGA curves are shown in Figures 2 and S1 in the Supporting Information (SI), respectively.

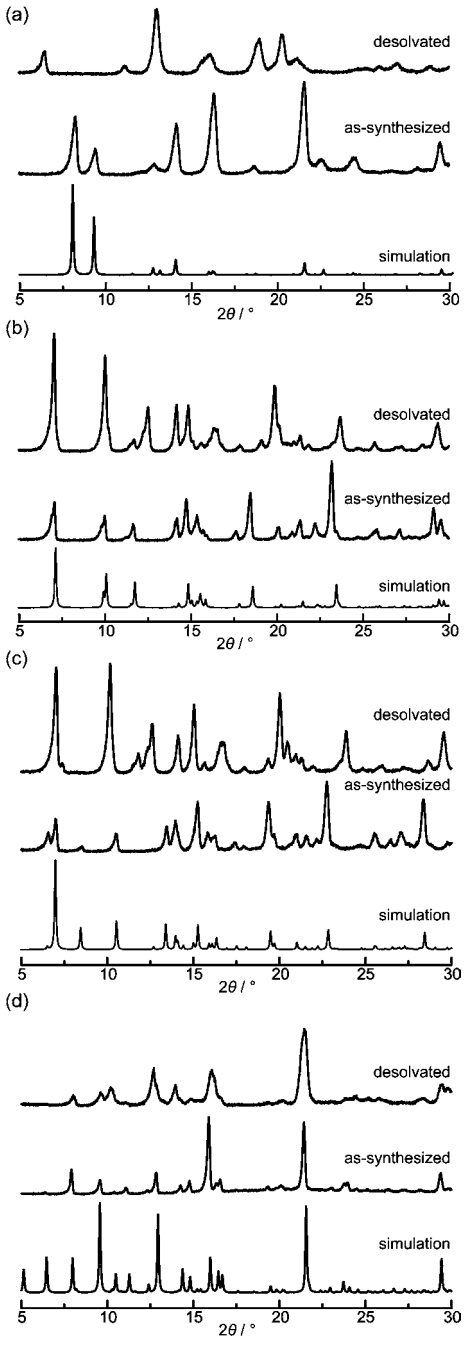


**Figure 2.** PXRD patterns of the simulated (lowest), as-synthesized (middle), and desolvated (highest) phases of **1** (a), **2** (b), **3** (c), and **4** (d).

The TGA curves of **1**−**3** clearly indicated accommodation of solvent molecules in the as-synthesized phase. A weight loss of 24% was observed in the TGA curve of **1**, and guest molecules were released above 130 to 150 °C, as shown in Figure S1a in the SI. Therefore, we removed guest molecules by evacuation at 150 °C for 6 h. While **1** in the as-synthesized phase showed a PXRD pattern similar to the simulated pattern produced from the single-crystal X-ray structure, the desolvated phase showed patterns different from those of the as-synthesized phase, as shown in Figure 2a. This difference indicates that **1** has structural flexibility. Desolvated **1** showed a broadening of the pattern and weaker intensity, which suggested partial collapse of the framework. The larger porosity of **1** causes the lower stability, and it collapsed completely above 380 °C. In the cases of **2** and **3**, each framework starts releasing DMF at around 100 °C, as shown in parts b and c of Figure S1 in the SI, respectively. The decrease of 17% in weight corresponds to the inclusion of ca. 2.5 DMF molecules per $Zn_2$ ($Zn_2$ means one paddle-wheel unit) in each framework. No weight loss of **2** was observed from 150 to 380 °C, and **2** collapses above 380 °C. In contrast, **3** showed two stepwise weight losses at around 290 and 400 °C. The former decrease indicates collapse of the framework because of the weaker coordination bond between $Zn^{2+}$ and bpt compared with bpb. On the basis of the TGA measurements, we could remove guest DMF molecules at 150 and 100 °C from **2** and **3**, respectively, without collapse. The PXRD patterns of **2** and **3** in the desolvated phase were different from those in the as-synthesized phase, as shown in Figures 2b,c, which means that they also have structural flexibility. Although the PXRD patterns of **2** and **3** are different in the as-synthesized phase, both **2** and **3** showed similar diffraction patterns in the desolvated phase. Therefore, we can assume that the desolvated structures of **2** and **3** are similar. We determined the crystal structure of **2** in the degassed phase by single-crystal X-ray analysis, and the PXRD pattern in the desolvated phase of **2** is not different largely from the simulated one in the degassed phase, as shown in Figure S2 in the SI. Consequently, **3** in the desolvated phase is similar to **2**. In the case of **4**, the framework showed a distinct TGA curve that was different from the others, as shown in Figure S1d in the SI. The TGA curve showed little weight decrease below 400 °C, which indicated that there was no guest molecule in **4** as a result of less void space than in the others, and the collapse happens above 400 °C. After evacuation of **4** at 150 °C for 3 h for confirmation of desolvation, a different behavior was not observed in the TGA curve. Both PXRD patterns in the as-synthesized and evacuated phases are quite similar, as shown in Figure 2d. Overall, **4** has no guest molecules and less flexibility compared with other frameworks. We were also attracted to the local dynamics of organic ligands in frameworks because some studies have implied that those dynamics relate to gas-adsorption processes.[23] The local dynamics of bpy were investigated using solid-state $^2$H NMR measurements of deuterated **4** (**4**-*d*). The typical Pake pattern of the $^2$H NMR spectrum obtained at 298 K is shown in Figure S3 in the SI. This narrow spectrum indicates that bpy is in a motional state despite the lower structural flexibility. The reason is that the motional state of bpy is spatially isolated from the restrictions of the surrounding organic ligands by the rhombic sdb ligands; therefore, bpy can move dynamically. This motion would disturb the rigidity of **4**, which showed a structural change when gas molecules were included at 298 K, as discussed later.


dx.doi.org/10.1021/ic302006x | *Inorg. Chem.* 2013, 52, 3634−3642

**$CO_2$ Adsorption Properties.** We investigated the adsorption behaviors of all four frameworks that have variable flexibility and different void spaces. We chose $CO_2$ as a probe gas molecule. The kinetic diameter of $CO_2$ is 3.3 Å,[4b] which is small enough to enter the pores of **1**−**4**.

The larger cross-sectional diameter of **1** is 6.6 Å for the rhombic grid along the dabco ligands, and those of **2** and **3** are also 6.6 Å along the bpt and bpb ligands. For **4**, the diameter of the 1D channel along the *c* axis is largest, 3.3 Å. Adsorption measurements of $CO_2$ were carried out up to $P/P_0$ = 1.0 at 195 K, shown in Figure 3. All of them start to take up $CO_2$ from the low-pressure region, and the amounts of $CO_2$ reached 66 mL·g$^{-1}$ in **1** (2.5 $CO_2$ per $Zn_2$), 137 mL·g$^{-1}$ in **2** (5.9 $CO_2$ per $Zn_2$), 141 mL·g$^{-1}$ in **3** (6.1 $CO_2$ per $Zn_2$), and 29 mL·g$^{-1}$ in **4** (1.2 $CO_2$ per $Zn_2$). Meanwhile, the void volume of **1** is the largest in the four frameworks; both **2** and **3** adsorbed twice the amounts of $CO_2$ as did **1**. This is because the gas-adsorption performance of **1** depends on the desolvation process. The tendency to adsorb lower amounts than expected from the single-crystal structure has often been observed in other adsorption measurements in this work. The framework of **4** adsorbed the least amount of $CO_2$, which is consistent with the smallest void volume of **4** in the four frameworks. The Brunauer−Emmett−Teller (BET) surface areas of these frameworks are shown in Table S1 in the SI. The surface area of **4** is the smallest. While the adsorption isotherms of **1** and **4** are categorized as type I isotherms, both **2** and **3** showed stepwise adsorption behaviors. The PXRD patterns of **2** and **3** in the desolvated phase are similar, and **2** and **3** showed similar adsorption isotherms up to $P$ = 25 kPa with structural changes supported by the diffraction patterns of **3** under a controlled pressure of $CO_2$ obtained using synchrotron irradiation, as shown in Figure S4 in the SI. The different behaviors were observed above $P$ = 25 kPa. The adsorption isotherm of **2** is more moderate in the step region from $P$ = 25 to 55 kPa than that of **3** above $P$ = 80 kPa, which suggests that the structural changes of **2** and **3** are gradual and abrupt in each step region, respectively. Further investigation to reveal the details of **2** and **3** used IR measurements for **2** and **3** under a controlled pressure of $CO_2$ at 195 K. The stretching of the sulfonyl groups in the sdb ligands shifted slightly lower from 1330 cm$^{-1}$ during an increase in the $CO_2$ pressure. The shifts of IR spectra are not large, although the O atoms on the sulfonyl groups are isolated in the crystal structures. Therefore, the shifts to lower wavenumber suggested that the rhombic grids in the 1D double chain shrank or swelled and that the space between the 2D sheets expanded less dramatically in the low-pressure region. Accompanying an increase of pressure from $P$ = 65 to 100 kPa, large changes of the synchrotron-radiation PXRD patterns were observed at $2\theta$ = 3−4°. These changes correspond to the expansion of **3** before and after the abrupt uptake. In the desorption process, **3** shows a hysteresis loop, which also suggested that **3** stays in a different phase when $CO_2$ molecules fully occupy the pore. The difference in the linker ligands contributes to the stepwise adsorption. That is, the linker ligand of bpt in **3** coordinates to $Zn^{2+}$ more weakly than does bpb in **2**.[16p,24] This is also suggested by the density functional theory calculation shown in Figures S5 and S6 and Table S2 in the SI. This weaker coordination bond contributes to the larger flexibility and allows larger structural change. As a consequence, both **2** and **3** accommodate similar amounts of $CO_2$ based on similar void volumes through different structural changes. We will discuss the isotherms of **4** later in comparison with the case of other gas molecules.

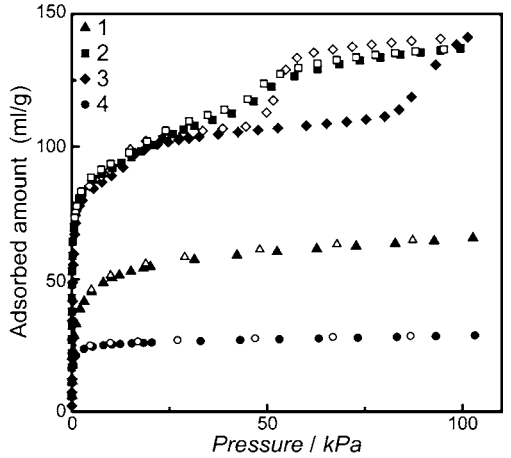


**Figure 3.** Adsorption isotherms of $CO_2$ at 195 K for **1**−**4**. Open and filled marks mean adsorption and desorption isotherms, respectively.

**$CH_4$ Adsorption Properties.** Shifts to higher wavenumber of $CO_2$ in the antisymmetric stretching mode were observed up to 2360 cm$^{-1}$ in Figure S7 in the SI, indicating interaction between $CO_2$ and the frameworks. In contrast, $CH_4$ molecules seem to interact less strongly with frameworks than $CO_2$ because of the nondipolar, nonquadrupolar, and isotropic

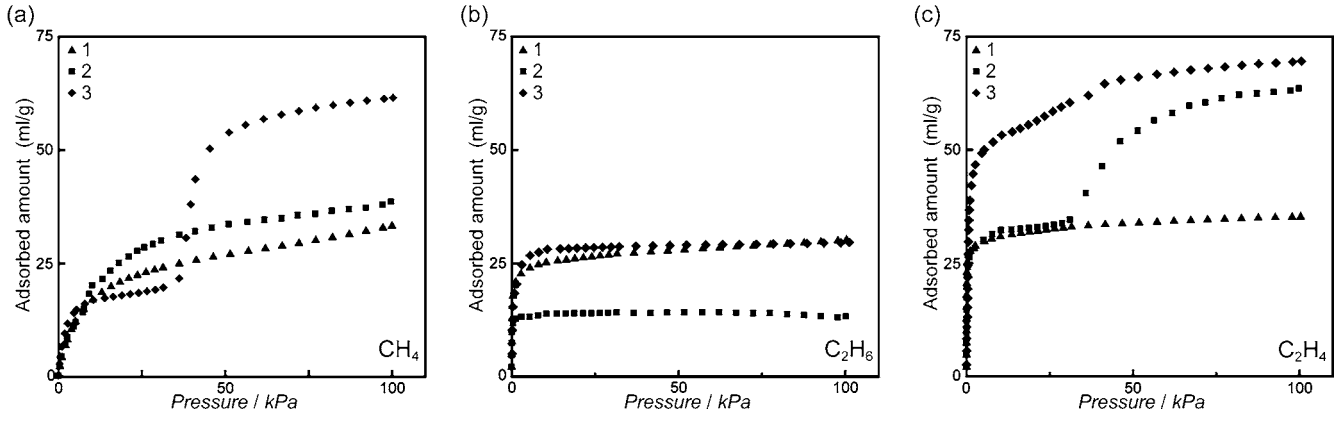


**Figure 4.** Adsorption isotherms of $CH_4$ (a), $C_2H_6$ (b), and $C_2H_4$ (c) at 195 K for **1**−**3**.


dx.doi.org/10.1021/ic302006x | Inorg. Chem. 2013, 52, 3634−3642

shape of $CH_4$. We can expect to obtain information on the intrinsic pore structures and framework flexibility using $CH_4$. Therefore, we carried out adsorption measurements of $CH_4$ up to $P$ = 101 kPa at 195 K. The kinetic diameter of $CH_4$ is 3.8 Å, which is larger than that of $CO_2$ (3.3 Å).[4b] The isotherms of $CH_4$ for **1**−**3** are shown in Figure 4a. The amount of adsorbed $CH_4$ in **1** is smallest, 33 mL·g$^{-1}$ (1.3 $CH_4$ per $Zn_2$), among the three frameworks. In contrast, **2** and **3** adsorbed larger amounts of $CH_4$, 39 mL·g$^{-1}$ (1.7 $CH_4$ per $Zn_2$) and 62 mL·g$^{-1}$ (2.7 $CH_4$ per $Zn_2$), respectively. Gradual uptake in **2** was observed, while stepwise adsorption in **3** occurred at $P$ = 38 kPa. Total uptakes of $CH_4$ in each framework were different up to $P$ = 101 kPa, although the capacity of both for $CO_2$ is similar. The stronger interaction of $CO_2$ than $CH_4$ generates the contrasting isotherm of **2**. For the case of **3**, the stepwise behavior and larger capacity suggested that the structural change was similar to the case of $CO_2$. The isotherm of $CH_4$ showed a more precipitous increase than that of $CO_2$. This behavior contributed to 68% of the total adsorbed $CH_4$, which is much larger than the 21% in the case of $CO_2$. $CH_4$ is larger than $CO_2$; therefore, $CH_4$ molecules forced **3** to expand the framework more at $P$ = 38 kPa, which was allowed by the more flexible coordination bonds between $Zn^{2+}$ and bpt in **3** compared with bpb in **2**. The different strengths of the coordination bond in **2** and **3** contribute to the various stepwise adsorption behaviors incorporating the diverse interactions of the gas molecules, $CO_2$ or $CH_4$.

**$C_2H_6$ Adsorption Properties.** The different flexibility of frameworks could offer fascinating adsorption properties depending on the properties of gases. We carried out adsorption measurements on a different nonpolar gas molecule with an anisotropic shape, $C_2H_6$, to investigate the size or shape dependence of the adsorption behavior in more detail. The kinetic diameter of $C_2H_6$ is 4.4 Å,[4b] which is larger than those of $CO_2$ and $CH_4$. The isotherms of $C_2H_6$ for **1**, **2**, and **3** up to $P$ = 101 kPa at 195 K are shown in Figure 4b. While **1** and **3** adsorbed 30 mL·g$^{-1}$ (1.1 $C_2H_6$ per $Zn_2$) and 30 mL·g$^{-1}$ (1.6 $C_2H_6$ per $Zn_2$) of $C_2H_6$, respectively, smaller amounts of $C_2H_6$, 13 mL·g$^{-1}$ (0.6 $C_2H_6$ per $Zn_2$), were accommodated in **2**. The trend of adsorption amounts of $C_2H_6$ is different from $CO_2$ or $CH_4$, and the least amount is adsorbed in **2** among the three frameworks. All of the isotherms were Type I profiles without any steps in the measurement region, which is also different from the isotherms of $CO_2$ and $CH_4$. The size and shape of $C_2H_6$ and protons on the central ring of bpb additionally contribute to these differences. Concerning the larger size of $C_2H_6$, the adsorbed amounts of $C_2H_6$ in **2** or **3** decreased. These lower amounts and decreased interaction compared with $CO_2$ could not induce large structural changes, even if they are flexible frameworks. In particular, both the anisotropic shape and the larger size of $C_2H_6$ effectively prevented **2** from adsorbing $C_2H_6$, and steric hindrance from the protons in bpb also contributed to the lower adsorption. Consequently, the accommodated volume of $C_2H_6$ in **2** was clearly decreased and the different behaviors between **2** and **3** were emphasized.

**$C_2H_4$ Adsorption Properties.** We also measured the adsorption isotherms of $C_2H_4$, which is similar to $C_2H_6$ in that they are both anisotropic. The kinetic diameter of $C_2H_4$ is 4.2 Å,[4b] which is larger than that of $CH_4$ and smaller than that of $C_2H_6$. $C_2H_4$ has a double bond, which provides a planar shape. $C_2H_4$ has an intermediate size, planar shape, and a double bond; therefore, it is suitable for comparison with the three other types of gas molecules. Furthermore, investigation of the adsorption behavior of these gases is important industrially, and their selective adsorption has been studied.[25] Isotherms of **1**−**3** up to $P$ = 101 kPa at 195 K are shown in Figure 4c. Their accommodated volumes are 35 mL·g$^{-1}$ in **1** (1.3 $C_2H_4$ per $Zn_2$), 64 mL·g$^{-1}$ in **2** (2.8 $C_2H_4$ per $Zn_2$), and 70 mL·g$^{-1}$ in **3** (3.0 $C_2H_4$ per $Zn_2$). The accommodated volume of $C_2H_4$ in **1** was similar to those of $CH_4$ and $C_2H_6$ because of their adequate void space. The $C_2H_4$ adsorption isotherm of **2** has an abrupt increase at $P$ = 31 kPa, which contrasts with the cases of $CH_4$ and $C_2H_6$ adsorption. Almost three $C_2H_4$ molecules are adsorbed per one zinc paddle-wheel unit in both **2** and **3**, although the protons of bpb in **2** decrease the void space for $C_2H_6$. In other words, these protons do not greatly affect the total capacities for $C_2H_4$, including the abrupt increase in the measurement region. This increase is caused by a structural change, as in the case of $CO_2$. Because both $CO_2$ and $C_2H_4$ have larger quadrupole moments than $C_2H_6$, they would induce a structural change. The electron-withdrawing tetrazine rings in **3** have a tendency to interact more with $C_2H_4$ than **2**,[26] therefore, a structural change is induced during the adsorption of $C_2H_4$ even in the lower pressure region around $P$ = 0.3 kPa, as shown in Figure S8 in the SI. As mentioned above, the flexible coordination bond between $Zn^{2+}$ and bpt plays a significant role in the structural change. Totally, $\pi$ electrons of $C_2H_4$ respond to the electron-withdrawing tetrazine rings of the linker ligands in **3**. The different structural flexibility between **2** and **3** is induced by the tetrazine rings.[16p,24] These factors effectively work on the adsorption properties.

**Adsorption Properties of 4.** The adsorption processes of **1**−**3** are not size-selective; however, the frameworks showed various adsorption behaviors depending on the functional groups in the organic linkers and the structural flexibility. On the other hand, many studies have been reported relating to gate-opening phenomena based on the flexibility of PCP frameworks that have potential applicability to materials for separating various gas molecules. The reason why the flexible frameworks from **1**−**3** do not show the gate-opening phenomenon is that they can adsorb gas molecules from the rhombic grids, which are permanent large pores, as shown in Figure 1a. From this point of view, we focused on bpy, which has a suitable length to construct an interpenetrated structure with a rhombic grid pore occupied by bpy in a neighboring framework. We investigated the adsorption properties of **4**, which has much less void volume and a smaller window than the three other frameworks. We show adsorption isotherms at 195 K up to $P$ = 101 kPa of $CH_4$, $C_2H_6$, $C_2H_4$, and $CO_2$ for comparison in Figure 5a. The adsorption amounts of $CH_4$, $C_2H_6$, and $C_2H_4$ are negligible amount, 7 mL·g$^{-1}$ (0.3 $C_2H_4$ per $Zn_2$) and 13 mL·g$^{-1}$ (0.5 $C_2H_6$ per $Zn_2$). The isotherm of $CO_2$ has a type I profile; in contrast, $CH_4$ is not adsorbed in **4**. Isotherms of $C_2H_6$ and $C_2H_4$ exhibited the gate-opening phenomenon at $P$ = 1 and 8 kPa, respectively, as shown in Figure S9a in the SI in a logarithmic scale. The pore diameter of **4** is 3.3 Å, as mentioned above. This size is appropriate for $CO_2$ molecules to diffuse and for $CH_4$ to be excluded, and their isotherms indicated reasonable size selectivity depending on their size. In contrast, $C_2H_6$ and $C_2H_4$ showed inconsistent adsorption behaviors with a size-selective adsorption because they are larger than $CO_2$, $CH_4$, and the pore diameter of **4**. We obtained structural information on **4** during gas adsorption from diffraction patterns by synchrotron irradiation shown in Figure S10 in the SI. Slight differences in the diffraction pattern were observed compared with the degassed phase and $P$ = 90


dx.doi.org/10.1021/ic302006x | Inorg. Chem. 2013, 52, 3634−3642

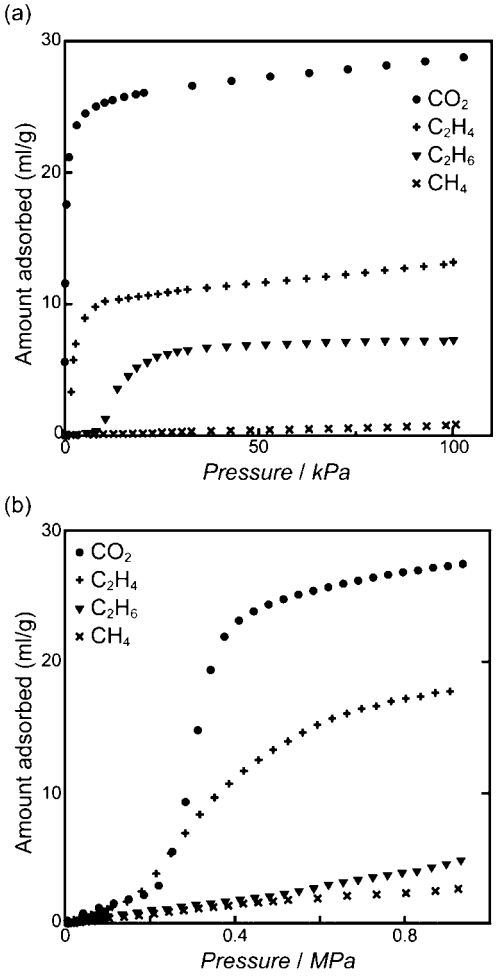


**Figure 5.** Adsorption isotherms of $CO_2$, $CH_4$, $C_2H_6$, and $C_2H_4$ at 195 K (a) and 298 K (b) for **4**.

kPa of $CO_2$ at 195 K, and little difference was observed in the degassed phase at 195, 298, and 423 K. In contrast, the dependence of the diffraction patterns on the temperature was clearly observed when $CO_2$ molecules were adsorbed under $P$ = 90 kPa from 195 to 298 K. We concluded that **4** has a small amount of structural flexibility independent of the $CO_2$ amounts at the same temperature, while the structure of **4** with $CO_2$ clearly depends on the temperature. When the framework of **4** is synthesized in a different way using an aqueous solution, water molecules are accommodated.[22] The simulated PXRD patterns of **4** at 223 K and **4**⊃$H_2O$ at 293 K are different, as shown in Figure S11 in the SI, which is consistent with the case of $CO_2$. The kinetic diameter of $H_2O$ is 2.6 Å, which is smaller than that of $CO_2$,[4b] and $H_2O$ accommodation induces a small amount of structural change more easily than does $CO_2$. In the cases of $C_2H_4$ and $C_2H_6$, they have quadrupole moments that are the same as that of $CO_2$ and tend to interact closely with the smaller pore of **4**. In this manner, we can surmise that a structural change is also induced slightly when $C_2H_4$ and $C_2H_6$ interact with the framework at 195 K and gate-opening adsorption occurred, although $C_2H_4$ and $C_2H_6$ are clearly larger than $H_2O$ or $CO_2$. The lower gate-opening pressure of $C_2H_4$ is derived from its chemical or physical properties, such as the double bond, molecular size, and larger quadrupole moment.

While the slight structural change of **4** shows selective or gate-opening adsorption at 195 K, the PXRD pattern greatly depends on the temperature under a $CO_2$ atmosphere at $P$ = 90 kPa, for instance at 195 and 298 K. Furthermore, the solid-state $^2H$ NMR spectrum indicates that bpy is in a motional state at 298 K. According to these behaviors, disturbance of the framework rigidity can be predicted at 298 K. Therefore, we performed adsorption measurements of those gas molecules to investigate their adsorption behaviors at 298 K. The adsorption isotherms up to $P$ = 0.9 MPa at 298 K are shown in Figure 5b. In the case of $CH_4$, the adsorbed amount is negligible at 298 K, the same as that at 195 K. The framework is found to be nonporous for $CH_4$ because of its intrinsic properties such as size and weak interaction. Clear gate-opening adsorption was absent in the isotherms of $C_2H_4$ and $C_2H_6$, as shown in Figure S9b in the SI in a logarithmic scale. A gradual uptake of $C_2H_6$ was observed, whereas the isotherm of $C_2H_4$ showed stepwise adsorption at $P$ = 0.12 MPa after adsorption of a certain amount. The stepwise adsorption is caused by a structural change because of the greater interaction of $C_2H_4$ than $C_2H_6$. As a result, the difference between the total amounts of adsorbed $C_2H_4$ and $C_2H_6$ increased in the measured pressure region. $CO_2$ was also adsorbed in a stepwise manner, similar to the $C_2H_4$ case; however, the adsorbed total amount of $CO_2$ is largest because of their sizes. We successfully introduced interpenetration involving a slight structural flexibility into the 2D-assembled framework of **4**. This framework exhibits various adsorption properties toward selective adsorption.

## CONCLUSIONS

We have demonstrated rational synthesis based on 2D-assembled frameworks using the sdb ligand, with four types of dinitrogen linker ligands, dabco, bpb, bpt, and bpy. They are a novel series of 2D frameworks, and a void space was introduced into the 1D double chain. The assembled structure and pore size are tuned by the length of the linker ligands. The shortest linker ligand, dabco, prevents interdigitation and interpenetration and generates the largest void space based on the single-crystal structure; however, we have not found the optimal condition for desolvation of **1** yet. The longer linker ligands, bpb and bpt, form interdigitated frameworks, and they showed stepwise adsorption properties depending on the structural flexibility of the frameworks and the properties of the gas molecules. An appropriately selected linker ligand, bpy, constructs quite small pores by interpenetration in 2D sheets having slight flexibility, and the PCP has gate-opening properties that depend on the gas molecules, even if there is no large structural flexibility. The local dynamics of spatially isolated bpy were also revealed. These approaches using 2D PCPs provide another strategy for selective adsorption.

## ASSOCIATED CONTENT

### Supporting Information

X-ray crystallographic data of **1**−**4** in the as-synthesized phase and **2** in the degassed phase in CIF format, TGA data of **1**−**4**, PXRD pattern of **2**, synchrotron PXRD patterns of **3** and **4** under a $CO_2$ atmosphere, BET surface areas of **1**−**4**, IR spectra of **2** and **3** under a $CO_2$ atmosphere, adsorption and desorption isotherms, calculated results of model structures with computational details, and solid-state $^2H$ NMR spectra of **4**-*d*. This material is available free of charge via the Internet at http://pubs.acs.org.


dx.doi.org/10.1021/ic302006x | *Inorg. Chem.* 2013, 52, 3634−3642

## AUTHOR INFORMATION


### Corresponding Author

*E-mail: kitagawa@icems.kyoto-u.ac.jp.


### Notes

The authors declare no competing financial interest.

## ACKNOWLEDGMENTS

This work was supported by the Japan Science and Technology Agency Precursory Research for Embryonic Science and Technology (PRESTO) program, by the Japan Science and Technology Agency Exploratory Research for Advanced Technology (ERATO) program, by Grants-in-Aid for Scientific Research, the Japan Society for the Promotion of Science (JSPS), and by the WPI-iCeMS Program. iCeMS is supported by the World Premier International Research Initiative (WPI), MEXT, Japan.

## REFERENCES


(1) (a) Kondo, M.; Yoshitomi, T.; Seki, K.; Matsuzaka, H.; Kitagawa, S. *Angew. Chem., Int. Ed.* **1997**, *36*, 1725. (b) Li, H.; Eddaoudi, M.; Groy, T. L.; Yaghi, O. M. *J. Am. Chem. Soc.* **1998**, *120*, 8571. (c) Mori, W.; Inoue, F.; Yoshida, K.; Nakayama, H.; Takamizawa, S.; Kishita, M. *Chem. Lett.* **1997**, 1219.

(2) (a) Kitagawa, S.; Kitaura, R.; Noro, S. *Angew. Chem., Int. Ed.* **2004**, *43*, 2334. (b) Furukawa, H.; Ko, N.; Go, Y. B.; Aratani, N.; Choi, S. B.; Choi, E.; Yazaydin, A. O.; Snurr, R. Q.; O'Keeffe, M.; Kim, J.; Yaghi, O. M. *Science* **2010**, *329*, 424. (c) Robinson, S. A. K.; Mempin, M. V. L.; Cairns, A. J.; Holman, K. T. *J. Am. Chem. Soc.* **2011**, *133*, 1634. (d) Wilmer, C. E.; Leaf, M.; Lee, C. Y.; Farha, O. K.; Hauser, B. G.; Hupp, J. T.; Snurr, R. Q. *Nat. Chem.* **2012**, *4*, 83.

(3) (a) Matsuda, R.; Kitaura, R.; Kitagawa, S.; Kubota, Y.; Belosludov, R. V.; Kobayashi, T. C.; Sakamoto, H.; Chiba, T.; Takata, M.; Kawazoe, Y.; Mita, Y. *Nature* **2005**, *436*, 238. (b) Millward, A. R.; Yaghi, O. M. *J. Am. Chem. Soc.* **2005**, *127*, 17998. (c) Wong-Foy, A. G.; Matzger, A. J.; Yaghi, O. M. *J. Am. Chem. Soc.* **2006**, *128*, 3494. (d) Dinca, M.; Dailly, A.; Liu, Y.; Brown, C. M.; Neumann, D. A.; Long, J. R. *J. Am. Chem. Soc.* **2006**, *128*, 16876. (e) Ma, S.; Sun, D.; Simmons, J. M.; Collier, C. D.; Yuan, D.; Zhou, H.-C. *J. Am. Chem. Soc.* **2008**, *130*, 1012.

(4) (a) Chen, B. L.; Liang, C. D.; Yang, J.; Contreras, D. S.; Clancy, Y. L.; Lobkovsky, E. B.; Yaghi, O. M.; Dai, S. *Angew. Chem., Int. Ed.* **2006**, *45*, 1390. (b) Li, J. R.; Kuppler, R. J.; Zhou, H. C. *Chem. Soc. Rev.* **2009**, *38*, 1477. (c) Li, J. R.; Sculley, J.; Zhou, H. C. *Chem. Rev.* **2012**, *112*, 869.

(5) (a) Seo, J. S.; Whang, D.; Lee, H.; Jun, S. I.; Oh, J.; Jeon, Y. J.; Kim, K. *Nature* **2000**, *404*, 982. (b) Uemura, T.; Hiramatsu, D.; Kubota, Y.; Takata, M.; Kitagawa, S. *Angew. Chem., Int. Ed.* **2007**, *46*, 4987. (c) El-Shall, M. S.; Abdelsayed, V.; Khder, A. E. R. S.; Hassan, H. M. A.; El-Kaderi, H. M.; Reich, T. E. *J. Mater. Chem.* **2009**, *19*, 7625. (d) Lee, J.; Farha, O. K.; Roberts, J.; Scheidt, K. A.; Nguyen, S. T.; Hupp, J. T. *Chem. Soc. Rev.* **2009**, *38*, 1450. (e) Yoon, M.; Srirambalaji, R.; Kim, K. *Chem. Rev.* **2012**, *112*, 1196.

(6) (a) Tanaka, D.; Horike, S.; Kitagawa, S.; Ohba, M.; Hasegawa, M.; Ozawa, Y.; Toriumi, K. *Chem. Commun.* **2007**, 3142. (b) Takashima, Y.; Martinez, V. M.; Furukawa, S.; Kondo, M.; Shimomura, S.; Uehara, H.; Nakahama, M.; Sugimoto, K.; Kitagawa, S. *Nat. Commun.* **2011**, *2*, 168. (c) Cui, Y. J.; Yue, Y. F.; Qian, G. D.; Chen, B. L. *Chem. Rev.* **2012**, *112*, 1126. (d) Maspoch, D.; Ruiz-Molina, D.; Wurst, K.; Domingo, N.; Cavallini, M.; Biscarini, F.; Tejada, J.; Rovira, C.; Veciana, J. *Nat. Mater.* **2003**, *2*, 190. (e) Ohba, M.; Yoneda, K.; Agusti, G.; Munoz, M. C.; Gaspar, A. B.; Real, J. A.; Yamasaki, M.; Ando, H.; Nakao, Y.; Sakaki, S.; Kitagawa, S. *Angew. Chem., Int. Ed.* **2009**, *48*, 4767. (f) Kurmoo, M. *Chem. Soc. Rev.* **2009**, *38*, 1353.

(7) (a) Kitagawa, H.; Nagao, Y.; Fujishima, M.; Ikeda, R.; Kanda, S. *Inorg. Chem. Commun.* **2003**, *6*, 346. (b) Bureekaew, S.; Horike, S.; Higuchi, M.; Mizuno, M.; Kawamura, T.; Tanaka, D.; Yanai, N.; Kitagawa, S. *Nat. Mater.* **2009**, *8*, 831. (c) Hurd, J. A.; Vaidhyanathan, R.; Thangadurai, V.; Ratcliffe, C. I.; Moudrakovski, I. L.; Shimizu, G. K. H. *Nat. Chem.* **2009**, *1*, 705. (d) Ohkoshi, S.; Nakagawa, K.; Tomono, K.; Imoto, K.; Tsunobuchi, Y.; Tokoro, H. *J. Am. Chem. Soc.* **2010**, *132*, 6620.

(8) (a) Wang, X.-S.; Meng, L.; Cheng, Q.; Kim, C.; Wojtas, L.; Chrzanowski, M.; Chen, Y.-S.; Zhang, X. P.; Ma, S. *J. Am. Chem. Soc.* **2011**, *133*, 16322. (b) Serre, C.; Millange, F.; Thouvenot, C.; Nogues, M.; Marsolier, G.; Louer, D.; Ferey, G. *J. Am. Chem. Soc.* **2002**, *124*, 13519. (c) Dybtsev, D. N.; Chun, H.; Kim, K. *Angew. Chem., Int. Ed.* **2004**, *43*, 5033.

(9) Horike, S.; Shimomura, S.; Kitagawa, S. *Nat. Chem.* **2009**, *1*, 695.

(10) (a) Bureekaew, S.; Sato, H.; Matsuda, R.; Kubota, Y.; Hirose, R.; Kim, J.; Kato, K.; Takata, M.; Kitagawa, S. *Angew. Chem., Int. Ed.* **2010**, *49*, 7660. (b) Kitaura, R.; Seki, K.; Akiyama, G.; Kitagawa, S. *Angew. Chem., Int. Ed.* **2003**, *42*, 428. (c) Kondo, A.; Noguchi, H.; Ohnishi, S.; Kajiro, H.; Tohdoh, A.; Hattori, Y.; Xu, W. C.; Tanaka, H.; Kanoh, H.; Kaneko, K. *Nano Lett.* **2006**, *6*, 2581.

(11) (a) Eddaoudi, M.; Kim, J.; Rosi, N.; Vodak, D.; Wachter, J.; O'Keeffe, M.; Yaghi, O. M. *Science* **2002**, *295*, 469. (b) Ma, B. Q.; Mulfort, K. L.; Hupp, J. T. *Inorg. Chem.* **2005**, *44*, 4912. (c) Chun, H.; Dybtsev, D. N.; Kim, H.; Kim, K. *Chem.—Eur. J.* **2005**, *11*, 3521. (d) Ma, L. Q.; Falkowski, J. M.; Abney, C.; Lin, W. B. *Nat. Chem.* **2010**, *2*, 838.

(12) (a) Dietzel, P. D. C.; Morita, Y.; Blom, R.; Fjellvag, H. *Angew. Chem., Int. Ed.* **2005**, *44*, 6354. (b) Rosi, N. L.; Kim, J.; Eddaoudi, M.; Chen, B. L.; O'Keeffe, M.; Yaghi, O. M. *J. Am. Chem. Soc.* **2005**, *127*, 1504. (c) Dietzel, P. D. C.; Panella, B.; Hirscher, M.; Blom, R.; Fjellvag, H. *Chem. Commun.* **2006**, 959. (d) Caskey, S. R.; Wong-Foy, A. G.; Matzger, A. J. *J. Am. Chem. Soc.* **2008**, *130*, 10870. (e) Bhattacharjee, S.; Choi, J. S.; Yang, S. T.; Choi, S. B.; Kim, J.; Ahn, W. S. *J. Nanosci. Nanotechnol.* **2010**, *10*, 135.

(13) (a) Devic, T.; Serre, C.; Audebrand, N.; Marrot, J.; Ferey, G. *J. Am. Chem. Soc.* **2005**, *127*, 12788. (b) Vitorino, M. J.; Devic, T.; Tromp, M.; Ferey, G.; Visseaux, M. *Macromol. Chem. Phys.* **2009**, *210*, 1923. (c) Devic, T.; Wagner, V.; Guillou, N.; Vimont, A.; Haouas, M.; Pascolini, M.; Serre, C.; Marrot, J.; Daturi, M.; Taulelle, F.; Ferey, G. *Microporous Mesoporous Mater.* **2011**, *140*, 25. (d) Reinsch, H.; Krüger, M.; Wack, J.; Senker, J.; Salles, F.; Maurin, G.; Stock, N. *Microporous Mesoporous Mater.* **2012**, *157*, 50.

(14) (a) Millange, F.; Serre, C.; Ferey, G. *Chem. Commun.* **2002**, 822. (b) Loiseau, T.; Serre, C.; Huguenard, C.; Fink, G.; Taulelle, F.; Henry, M.; Bataille, T.; Ferey, G. *Chem.—Eur. J.* **2004**, *10*, 1373. (c) Whitfield, T. R.; Wang, X. Q.; Liu, L. M.; Jacobson, A. J. *Solid State Sci.* **2005**, *7*, 1096. (d) Volkringer, C.; Loiseau, T.; Guillou, N.; Ferey, G.; Elkaim, E.; Vimont, A. *Dalton Trans.* **2009**, 2241. (e) Anokhina, E. V.; Vougo-Zanda, M.; Wang, X. Q.; Jacobson, A. J. *J. Am. Chem. Soc.* **2005**, *127*, 15000. (f) Devic, T.; Horcajada, P.; Serre, C.; Salles, F.; Maurin, G.; Moulin, B.; Heurtaux, D.; Clet, G.; Vimont, A.; Greneche, J. M.; Le Ouay, B.; Moreau, F.; Magnier, E.; Filinchuk, Y.; Marrot, J.; Lavalley, J. C.; Daturi, M.; Ferey, G. *J. Am. Chem. Soc.* **2010**, *132*, 1127. (g) Barthelet, K.; Marrot, J.; Riou, D.; Ferey, G. *Angew. Chem., Int. Ed.* **2001**, *41*, 281.

(15) (a) Fujita, M.; Kwon, Y. J.; Washizu, S.; Ogura, K. *J. Am. Chem. Soc.* **1994**, *116*, 1151. (b) Subramanian, S.; Zaworotko, M. J. *Angew. Chem., Int. Ed.* **1995**, *34*, 2127. (c) Tong, M. L.; Ye, B. H.; Cai, J. W.; Chen, X. M.; Ng, S. W. *Inorg. Chem.* **1998**, *37*, 2645. (d) Zhang, Y. S.; Enright, G. D.; Breeze, S. R.; Wang, S. N. *New J. Chem.* **1999**, *23*, 625. (e) Noro, S.; Kitagawa, S.; Kondo, M.; Seki, K. *Angew. Chem., Int. Ed.* **2000**, *39*, 2082. (f) Noro, S.; Kitaura, R.; Kondo, M.; Kitagawa, S.; Ishii, T.; Matsuzaka, H.; Yamashita, M. *J. Am. Chem. Soc.* **2002**, *124*, 2568. (g) Kondo, A.; Noguchi, H.; Carlucci, L.; Proserpio, D. M.; Ciani, G.; Kajiro, H.; Ohba, T.; Kanoh, H.; Kaneko, K. *J. Am. Chem. Soc.* **2007**, *129*, 12362. (h) Kajiro, H.; Kondo, A.; Kaneko, K.; Kanoh, H. *Int. J. Mol. Sci.* **2010**, *11*, 3803.

(16) (a) Ma, C. B.; Chen, C. N.; Liu, Q. T.; Liao, D. H.; Li, L.; Sun, L. C. *New J. Chem.* **2003**, *27*, 890. (b) Tao, J.; Chen, X. M.; Huang, R. B.; Zheng, L. S. *J. Solid State Chem.* **2003**, *170*, 130. (c) Choi, E. Y.; Kwon, Y. U. *Inorg. Chem. Commun.* **2004**, *7*, 942. (d) Bradshaw, D.;

Rosseinsky, M. J. *Solid State Sci.* **2005**, *7*, 1522. (e) Wen, Y. H.; Cheng, H. K.; Feng, Y. L.; Zhang, H.; Li, Z. H.; Yao, Y. G. *Inorg. Chim. Acta* **2005**, *358*, 3347. (f) Tian, G.; Zhu, G. S.; Fang, Q. R.; Guo, X. D.; Xue, M.; Sun, J. Y.; Qiu, S. L. *J. Mol. Struct.* **2006**, *787*, 45. (g) Horike, S.; Tanaka, D.; Nakagawa, K.; Kitagawa, S. *Chem. Commun.* **2007**, 3395. (h) Tanaka, D.; Nakagawa, K.; Higuchi, M.; Horike, S.; Kubota, Y.; Kobayashi, L. C.; Takata, M.; Kitagawa, S. *Angew. Chem., Int. Ed.* **2008**, *47*, 3914. (i) Ma, L. F.; Wang, L. Y.; Wang, Y. Y.; Batten, S. R.; Wang, J. G. *Inorg. Chem.* **2009**, *48*, 915. (j) Hulvey, Z.; Furman, J. D.; Turner, S. A.; Tang, M.; Cheetham, A. K. *Cryst. Growth Des.* **2010**, *10*, 2041. (k) Nadeem, M. A.; Bhadbhade, M.; Bircher, R.; Stride, J. A. *Cryst. Growth Des.* **2010**, *10*, 4060. (l) Sato, H.; Matsuda, R.; Sugimoto, K.; Takata, M.; Kitagawa, S. *Nat. Mater.* **2010**, *9*, 661. (m) Nakagawa, K.; Tanaka, D.; Horike, S.; Shimomura, S.; Higuchi, M.; Kitagawa, S. *Chem. Commun.* **2010**, *46*, 4258. (n) Fukushima, T.; Horike, S.; Inubushi, Y.; Nakagawa, K.; Kubota, Y.; Takata, M.; Kitagawa, S. *Angew. Chem., Int. Ed.* **2010**, *49*, 4820. (o) Takashima, Y.; Furukawa, S.; Kitagawa, S. *CrystEngComm* **2011**, *13*, 3360. (p) Hijikata, Y.; Horike, S.; Sugimoto, M.; Sato, H.; Matsuda, R.; Kitagawa, S. *Chem.—Eur. J.* **2011**, *17*, 5138. (q) Hirai, K.; Uehara, H.; Kitagawa, S.; Furukawa, S. *Dalton Trans.* **2012**, *41*, 3924. (r) Sato, H.; Matsuda, R.; Mir, M. H.; Kitagawa, S. *Chem. Commun.* **2012**, *48*, 7919. (s) Kishida, K.; Horike, S.; Nakagawa, K.; Kitagawa, S. *Chem. Lett.* **2012**, *41*, 425. (t) Fukushima, T.; Horike, S.; Kobayashi, H.; Tsujimoto, M.; Isoda, S.; Foo, M. L.; Kubota, Y.; Takata, M.; Kitagawa, S. *J. Am. Chem. Soc.* **2012**, *134*, 13341.

(17) (a) Xiao, D. R.; Li, Y. G.; Wang, E. B.; Fan, L. L.; An, H. Y.; Su, Z. M.; Xu, L. *Inorg. Chem.* **2007**, *46*, 4158. (b) Furukawa, H.; Kim, J.; Ockwig, N. W.; O'Keeffe, M.; Yaghi, O. M. *J. Am. Chem. Soc.* **2008**, *130*, 11650. (c) Lin, J. D.; Long, X. F.; Lin, P.; Du, S. W. *Cryst. Growth Des.* **2010**, *10*, 146. (d) Zhuang, W. J.; Sun, H. L.; Xu, H. B.; Wang, Z. M.; Gao, S.; Jin, L. P. *Chem. Commun.* **2010**, *46*, 4339. (e) Kundu, T.; Sahoo, S. C.; Banerjee, R. *Chem. Commun.* **2012**, *48*, 4998. (f) Yeh, C. T.; Lin, W. C.; Lo, S. H.; Kao, C. C.; Lin, C. H.; Yang, C. C. *CrystEngComm* **2012**, *14*, 1219. (g) Bisht, K. K.; Suresh, E. *Inorg. Chem.* **2012**, *51*, 9577.

(18) Han, Y. F.; Lin, Y. J.; Jia, W. G.; Jin, G. X. *Organometallics* **2008**, *27*, 4088.

(19) Yamamoto, M.; Oshima, K.; Matsubara, S. *Heterocycles* **2006**, *67*, 353.

(20) Spek, A. L. *J. Appl. Crystallogr.* **2003**, *36*, 7.

(21) Vandersluis, P.; Spek, A. L. *Acta Crystallogr., Sect. A* **1990**, *46*, 194.

(22) (a) Li, N.; Chen, L.; Lian, F. Y.; Jiang, F. L.; Hong, M. C. *Chin. J. Struct. Chem.* **2009**, *28*, 1417. (b) Wang, J. Y.; Zhang, Y.; Ji, Y. Y. *Solid State Sci.* **2009**, *11*, 364. (c) Zhuang, W. J.; Sun, C. Y.; Jin, L. P. *Polyhedron* **2007**, *26*, 1123.

(23) (a) Hijikata, Y.; Horike, S.; Tanaka, D.; Groll, J.; Mizuno, M.; Kim, J.; Takata, M.; Kitagawa, S. *Chem. Commun.* **2011**, *47*, 7632. (b) Cussen, E. J.; Claridge, J. B.; Rosseinsky, M. J.; Kepert, C. J. *J. Am. Chem. Soc.* **2002**, *124*, 9574. (c) Horike, S.; Matsuda, R.; Tanaka, D.; Matsubara, S.; Mizuno, M.; Endo, K.; Kitagawa, S. *Angew. Chem., Int. Ed.* **2006**, *45*, 7226. (d) Amirjalayer, S.; Tafipolsky, M.; Schmid, R. *Angew. Chem., Int. Ed.* **2007**, *46*, 463. (e) Takamizawa, S.; Nataka, E.; Akatsuka, T.; Miyake, R.; Kakizaki, Y.; Takeuchi, H.; Maruta, G.; Takeda, S. *J. Am. Chem. Soc.* **2010**, *132*, 3783.

(24) Matsuda, R.; Tsujino, T.; Sato, H.; Kubota, Y.; Morishige, K.; Takata, M.; Kitagawa, S. *Chem. Sci.* **2010**, *1*, 315.

(25) (a) Baker, R. W. *Ind. Eng. Chem. Res.* **2002**, *41*, 1393. (b) Gucuyener, C.; van den Bergh, J.; Gascon, J.; Kapteijn, F. *J. Am. Chem. Soc.* **2010**, *132*, 17704. (c) van den Bergh, J.; Gucuyener, C.; Pidko, E. A.; Hensen, E. J. M.; Gascon, J.; Kapteijn, F. *Chem.—Eur. J.* **2011**, *17*, 8832. (d) Nijem, N.; Wu, H. H.; Canepa, P.; Marti, A.; Balkus, K. J.; Thonhauser, T.; Li, J.; Chabal, Y. J. *J. Am. Chem. Soc.* **2012**, *134*, 15201.

(26) (a) Domingo, L. R.; Picher, M. T.; Saez, J. A. *J. Org. Chem.* **2009**, *74*, 2726. (b) Chen, C.; Allen, C. A.; Cohen, S. M. *Inorg. Chem.* **2011**, *50*, 10534.